Particle Motion Near a Ring

D. J. Scheeres
Jet Propulsion Laboratory
Ca ifornia Institute of Technology
Pasadena, CA

Keywords: ring stability, ing growth, Hill's Equation of motion, periodic or its, n-body problem

Abstract

The dynamics of a particle moving near a classical ring is studied under a Hill-type approximation. A classical ring is comprised of particles of equal mass arranged symmetrically about a massive central body, tile particles having a uniform rotation rate. Two distinct equations of motion are found which describe the motion of a particle near such a ring. The fundamentals of each set are studied. Then a family of symmetric, planar periodic orbits arc computed. Finally, using the analysis of the derived equations of motion, a mechanism is conjectured which describes how a ring may gain mass. This mechanism is appealing as it is self-limiting and ceases to exist when the ring is still stable, yet more massive than its initial configuration.

1 Introduction

The motion of a material point is investigated under the attraction of a "classical" ring. A classical ring being a system comprised of P ring particles of equal mass arranged symmetrically about a central body, the entire ring having some specified rotation rate. Such a ring may be stable if the mass of each ring particle is small enough as compared to the central body mass (Reference [1 3]). There has been recent and historical interest in this simple model of a ring (References [8], [1 O], [12], [13], [14], [18], [9]), driven in part by the symmetry of the ring and its simple specification. The current problem of the motion of a material point under the attraction of such a ring has been investigated earlier (Reference [14]) when the ring is comprised of a finite number of particles. The current analysis deals with a particular approximation which simplifies the earlier study and brings out significant results. The approximation introduced here is a variant, of the Hill approximation first used by Hill in the three-body problem to study the motion of the 1110011. The approximation assumes that the satellite and ring arc close to each other, that the central body mass dominates the system and that the number of ring particles is large. After application of the approximation the system consists of a line of equally spaced ring particles extending to infinity. The actuations of motion contain gyroscopic terms and retain the major effect of the central body.

In deriving the approximate equations two special cases arc found. The first case results in equations of motion directly related to the classical hill equations of motion for the moon. The second case is unique and has an interesting and useful interpretation and application to motion near a ring. The two cases arc related by a transformation which is singular for certain parameter values. The basic dynamical properties of each case arc discussed. Then a family of periodic orbits in the second case is studied numerically. The stability properties of these orbits indicate the presence of regions of stable and unstable orbits adjacent to the ring. Finally, in analyzing the results a possible self-lilllitiag mechanism for ring growth is identified.

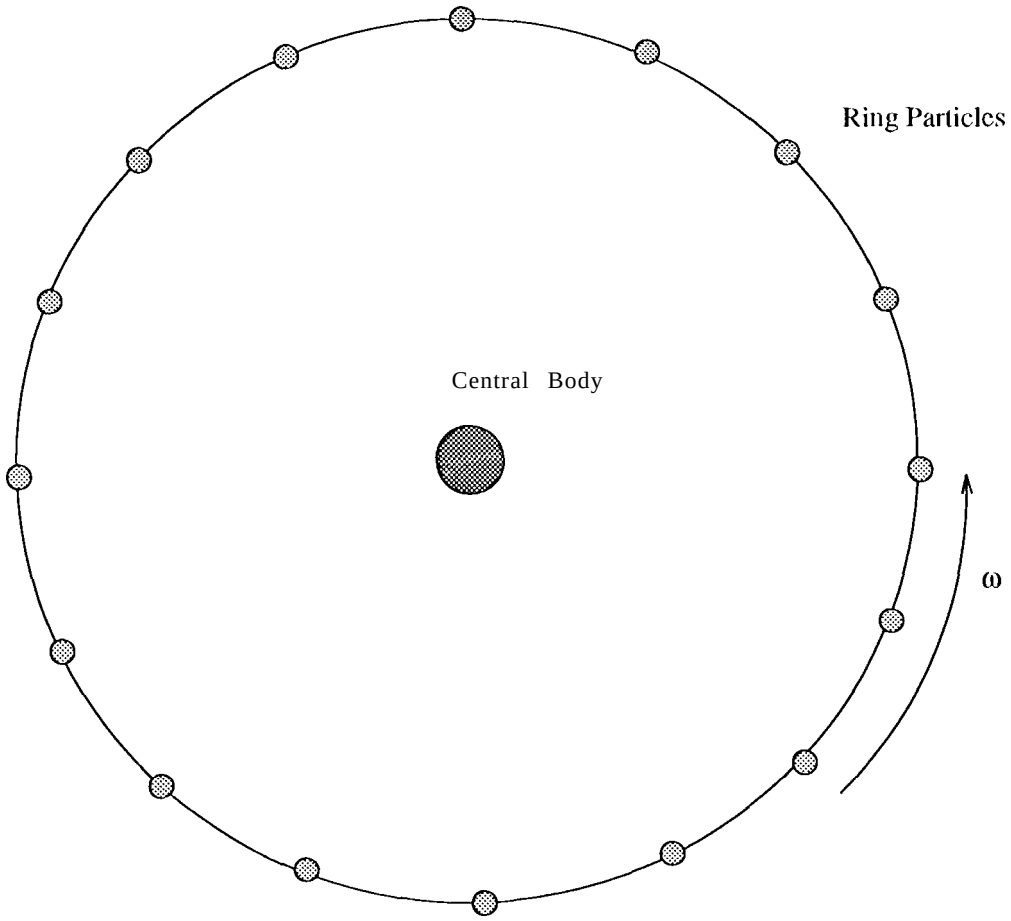

Figure 1: Geometrical Representation of the 1' l'article Ring

2 Equations of Motion

Consider the equations of motion of a massless particle M as attracted by a central body of unit mass and a ring with 1' particles of equal mass μ equally spaced about the central body at a unit distance. A rigorous derivation of the equations of motion in this case can be found in Reference [16], Chapter II.

$$\ddot{\mathbf{r}} + \boldsymbol{\Omega} \times (2\dot{\mathbf{r}} + \boldsymbol{\Omega} \times \mathbf{r}) = \frac{\partial U}{\partial \mathbf{r}}, \tag{1}$$

$$U = \frac{1}{|\mathbf{r}|} + \mu \sum_{j=1}^{P} \left[\frac{1}{|\mathbf{r}_j - \mathbf{r}|} - \frac{\mathbf{r} \cdot \mathbf{r}_j}{|\mathbf{r}_j|^3} \right] \tag{2}$$

The vectors $\mathbf{r}_j$ denote the positions of the ring particles, the vector $\mathbf{r}$ denotes the position of the particle M. $\boldsymbol{\Omega}$ is the constant magnitude angular velocity vector of the coordinate system.

The P ring particles are assumed to be in a relative equilibrium configuration with respect to themselves and the central body. Assuming that the central body is at the center of mass of this

system, the relative equilibrium solution of the ring is defined as:

$$\mathbf{r}_j = \mathbf{R}_j^* \tag{3}$$
$$j = 1, 2, \ldots, 1'$$
$$|\Omega| = \omega \tag{4}$$
$$\omega^2 = 1 + \frac{\mu}{4} \sum_{k=0}^{P-1} \csc(k\theta). \tag{5}$$

The vectors $\mathbf{R}_j^*$ have the properties:

$$|\mathbf{R}_j^*| = 1 \tag{6}$$
$$\mathbf{R}_j^* \cdot \mathbf{R}_k^* = \cos 2\theta(k-j) \tag{7}$$
$$|\mathbf{R}_j^* - \mathbf{R}_k^*| = 2|\sin\ \theta(k-j)| \tag{8}$$
$$\mathbf{R}_{P+j}^* = \mathbf{R}_j^*. \tag{9}$$

The parameter ω is the rotation rate of the ring and $\theta = \pi/P$ is the vertex half-angle of the P-polygon which the ring describes. Such a ring is stable against linear perturbation if the mass of each ring particle is small enough ([13]):

$$\mu \leq \mu_S \tag{10}$$
$$\mu_S = \frac{16}{7\zeta(3)} \frac{1}{13 + 4\sqrt{10}} \theta^3 + \cdots \tag{11}$$
$$\approx 2.298\ldots/P^3. \tag{12}$$

Where:

$$\zeta(n) = \sum_{k=1}^{\infty} \frac{1}{k^n} \tag{13}$$
$$\zeta(3) = 1.202057\ldots. \tag{14}$$

The function $\zeta(n)$ is the Riemann Zeta function.

Note that $\sum_{j=1}^{P} \mathbf{R}_j^* = 0$ and discard the final term in the summation of Equation 2. Use property 9 to renumber the summation in Equation 2 over the integers:

$$j = -r_1, -r_1 + 1, \ldots, -1, 0, 1, \ldots, r_2 - 1, r_2 \tag{15}$$

where if $P = 2r$ then $r_1 = r$ and $r_2 = r - 1$, and if $P = 2r + 1$ then $r_1 = r_2 = r$. The vector equations of motion then become:

$$\ddot{\mathbf{r}} + \Omega \times (2\dot{\mathbf{r}} + \Omega \times \mathbf{r}) = -\frac{\mathbf{r}}{|\mathbf{r}|^3} + \mu \sum_{j=-r_1}^{r_2} \frac{\mathbf{R}_j^* - \mathbf{r}}{|\mathbf{R}_j^* - \mathbf{r}|^3}. \tag{16}$$

3 The Hill Approximation

These equations will be studied under the assumption that the body M remains close to the ring. This assumption is formalized by introducing the Hill approximation.

The Hill approximation is applicable to three-or-more-body systems with a few basic characteristics: that there is a massive body, about which orbit, a number of bodies with small mass; that (some of) these bodies with small mass are relatively close to each other; and usually that the center of mass of the small bodies follows a circular orbit around the larger body. A general application of this approximation to n-body systems is given in Reference [1 5]. Under the

approximation, the full attraction of the small bodies on each other is usually retained. By being close to a circular orbit about the central body, the net attractive and centrifugal forces nullify each other in the vicinity of the small bodies, the tidal force then arises from the mismatch between these cancellations, The approximation ignores the parallax of the central body with respect to the small bodies.

The hill approximation as described above does not fit the current system, since the small body system (ring plus the massless body) has its center of mass co-located with the central body and the ring particles may be far from each other. However with modification the approximation is applicable to the current system.

Without loss of generality, give a special status to the ring particle located by the vector $\mathbf{R}_P^*$. Transform the coordinate system of the equations of motion so they are centered on this particle. Enforce the condition that the satellite is close to the ring by introducing a scaling factor $\chi\mu^{1/3}$, where μ is the mass of each ring particle and $\mu \ll 1$ is assumed:

$$\mathbf{r} = \mathbf{R}_P^* + \chi\mu^{1/3}\hat{\mathbf{r}}. \tag{17}$$

The factor χ is an arbitrary scaling factor to be specified later.

Recall that $\mathbf{R}_P^*$ is a relative equilibrium solution in the rotating reference frame, hence $\dot{\mathbf{R}}_P^* = \ddot{\mathbf{R}}_P^* = 0$ and:

$$\boldsymbol{\Omega} \times (\boldsymbol{\Omega} \times \mathbf{R}_P^*) = -\omega^2 \mathbf{R}_P^*. \tag{18}$$

Substitute Transformation 17 into Equation 16:

$$\begin{aligned}\chi\mu^{1/3}\left[\ddot{\hat{\mathbf{r}}} + \boldsymbol{\Omega} \times \left(2\dot{\hat{\mathbf{r}}} + \boldsymbol{\Omega} \times \hat{\mathbf{r}}\right)\right] &= \omega^2 \mathbf{R}_P^* - \frac{\mathbf{R}_P^* + \chi\mu^{1/3}\hat{\mathbf{r}}}{|\mathbf{R}_P^* + \chi\mu^{1/3}\hat{\mathbf{r}}|^3} - \frac{\chi\mu^{1/3}}{\chi^3}\frac{\hat{\mathbf{r}}}{|\hat{\mathbf{r}}|^3} \\ &\quad + \mu \sum_{j=-r_1}^{r_2}{}' \frac{\mathbf{R}_j^* - \mathbf{R}_P^* - \chi\mu^{1/3}\hat{\mathbf{r}}}{|\mathbf{R}_j^* - \mathbf{R}_P^* - \chi\mu^{1/3}\hat{\mathbf{r}}|^3}.\end{aligned} \tag{19}$$

The notation $\sum_{k=r_1}^{r_2}{}' = \sum_{k=r_1, k\neq 0}^{r_2}$ is used.

in the classical application of the Hill approximation the summation term is not present, ([19], Chapter VI, §498-493). Using $|\mathbf{R}_P^*| = 1$ and $\mu^{1/3} \ll 1$, note the following expansion:

$$\frac{\mathbf{R}_P^* + \chi\mu^{1/3}\hat{\mathbf{r}}}{|\mathbf{R}_P^* + \chi\mu^{1/3}\hat{\mathbf{r}}|^3} = \mathbf{R}_P^* + \chi\mu^{1/3}[\hat{\mathbf{r}} - 3\mathbf{R}_P^*(\mathbf{R}_P^* \cdot \hat{\mathbf{r}})] + \mathcal{O}(\chi^2\mu^{2/3}). \tag{20}$$

The terms of order $\mu^{2/3}$ contain the parallax. Substitute Equation 20 into the Equation 19 and note that $(\omega^2 - 1)\mathbf{R}_P^* = \mathcal{O}(\mu)$ and hence is grouped with the higher order terms. Then divide by $\chi\mu^{1/3}$ to find:

$$\begin{aligned}\ddot{\hat{\mathbf{r}}} + \boldsymbol{\Omega} \times \left(2\dot{\hat{\mathbf{r}}} + \boldsymbol{\Omega} \times \hat{\mathbf{r}}\right) &= -\hat{\mathbf{r}} + 3\mathbf{R}_P^*(\mathbf{R}_P^* \cdot \hat{\mathbf{r}}) - \frac{\hat{\mathbf{r}}}{\chi^3 |\hat{\mathbf{r}}|^3} \\ &\quad + \frac{\mu^{2/3}}{\chi} \sum_{j=-r_1}^{r_2}{}' \frac{\mathbf{R}_j^* - \mathbf{R}_P^* - \chi\mu^{1/3}\hat{\mathbf{r}}}{|\mathbf{R}_j^* - \mathbf{R}_P^* - \chi\mu^{1/3}\hat{\mathbf{r}}|^3} + \mathcal{O}(\chi\mu^{1/3}).\end{aligned} \tag{21}$$

The expansion used in Equation 20 is not applicable to the summation term in Equation 21 as $|\mathbf{R}_j^* - \mathbf{R}_P^*| = 2|\sin\theta k|$ and may be arbitrarily small for θ small (P large). 'There is a dichotomy here as some of the ring particles are far enough away to have less than $\mathcal{O}(\chi\mu^{1/3})$ influence, yet others may be close enough to have a significant, influence. This is dealt with in the following section. Formally, the Hill approximation is completed by aking the limit $\mu \to 0$, the higher order terms then disappearing.

4 Modification of the Ring Potential

In this section the ring force term is studied:

$$\frac{\mu^{2/3}}{\chi} \sum_{j=-r_1}^{\infty}{}' \frac{\mathbf{R}_j^* - \mathbf{R}_P^* - \chi\mu^{1/3}\hat{\mathbf{r}}}{|\mathbf{R}_j^* - \mathbf{R}_P^* - \chi\mu^{1/3}\hat{\mathbf{r}}|^3}. \tag{22}$$

Its limiting form will be found as $\mu \to 0$.

Introduce a Cartesian realization of the vectors involved:

$$\mathbf{R}_k^* = \cos 2\theta k\hat{\mathbf{i}} + \sin 2\theta k\hat{\mathbf{j}} \tag{23}$$

$$\hat{\mathbf{r}} = \hat{x}\hat{\mathbf{i}} + \hat{y}\hat{\mathbf{j}} + \hat{z}\hat{\mathbf{k}}. \tag{24}$$

Introduce an assumption on the mass of the ring particles μ:

$$\mu = \sigma\theta^3 \tag{25}$$

$$\theta = \frac{\pi}{P} \tag{26}$$

where σ is not necessarily small. This assumption is reasonable as all the relevant, limits on μ presented earlier and found elsewhere have been of this general functional form (References [8], [13], [14], [18]). This scaling allows for discussion) of the local geometry of the ring in the vicinity of $\mathbf{R}_P^*$, independent of the number of ring particles. For a stable ring, the bound on σ is:

$$\sigma \leq \sigma_S \tag{27}$$

$$\sigma_S = \frac{16}{7(13 + 4/10)((3)} \tag{28}$$

$$= 0.0741352 \ldots .$$

Introduce the Cartesian realizations and the new form of μ into Equation 22 to find three scalar expressions for the ring fore.c:

$$F_{\hat{x}} = -\frac{1}{\chi^3} \sum_{k=-r_1}^{r_2}{}' \frac{\hat{x} + \frac{2\sin^2\theta k}{\sigma^{1/3}\chi\theta}}{|\mathbf{r}_k|^3} \tag{29}$$

$$F_{\hat{y}} = -\frac{1}{\chi^3} \sum_{k=-r_1}^{r_2}{}' \frac{\hat{y} - \frac{2\sin\theta k\cos\theta k}{\sigma^{1/3}\chi\theta}}{|\mathbf{r}_k|^3} \tag{30}$$

$$F_{\hat{z}} = -\frac{1}{\chi^3} \sum_{k=-r_1}^{r_2}{}' \frac{\hat{z}}{|\mathbf{r}_k|^3} \tag{31}$$

where

$$|\mathbf{r}_k| = \sqrt{\frac{4\sin^2\theta k}{\sigma^{2/3}\chi^2\theta^2} - \frac{4\sin\theta k}{\sigma^{1/3}\chi\theta}(\hat{y}\cos\theta k - \hat{x}\sin\theta k) + \hat{x}^2 + \hat{y}^2 + \hat{z}^2} \tag{32}$$

The above equations are now formally of the same order as the other terms in Equations 21.

As χ and σ remain non-zero as $\mu \to 0$, this implies that $\theta \to 0$ $(P \to \infty)$. Application of this limit will send the higher order terms $\mathcal{O}(\chi\sigma^{1/3}\theta)$ in Equation 21 to zero. Introduction of this formal limit then yields the modified form of the equations. In applying the limit assume that k is a fixed integer, then:

$$\lim_{\theta\to 0} \frac{\sin\theta k}{\theta} = k. \tag{33}$$

This limit is assumed to be true for all k. However, for arbitrarily large k (on the order of $P/2$), this is not a good assumption by itself. However, it may properly be applied to these equations. See Appendix A for a rigorous discussion of this and application of the limiting process to the ring force equations.

After application of the limit the force terms become:

$$F_{\hat{x}} = -\frac{1}{\chi^3}\sum_{k=-\infty}^{\infty}{}' \frac{\hat{x}}{\left[\hat{x}^2 + \left(\frac{2k}{\chi\sigma^{1/3}} - \hat{y}\right)^2 + \hat{z}^2\right]^{3/2}} \tag{34}$$

$$F_{\hat{y}} = -\frac{1}{\chi^3}\sum_{k=-\infty}^{\infty}{}' \frac{\hat{y} - \frac{2k}{\sigma^{1/3}\chi}}{\left[\hat{x}^2 + \left(\frac{2k}{\chi\sigma^{1/3}} - \hat{y}\right)^2 + \hat{z}^2\right]^{3/2}} \tag{35}$$

$$F_{\hat{z}} = -\frac{1}{\chi^3}\sum_{k=-\infty}^{\infty}{}' \frac{\hat{z}}{\left[\hat{x}^2 + \left(\frac{2k}{\chi\sigma^{1/3}} - \hat{y}\right)^2 + \hat{z}^2\right]^{3/2}} \tag{36}$$

where all the summations are convergent.

5 Approximate Equations of Motion

Apply the Cartesian realization to Equations 21 and introduce the modified ring force terms from Equations 34, 35 and 36. Note that $\boldsymbol{\Omega} \times (\boldsymbol{\Omega} \times \hat{\mathbf{r}}) = -\hat{\mathbf{r}} + \hat{z}\hat{\mathbf{k}} + \mathcal{O}(\mu)$ and $\mathbf{R}_P^* = \hat{\mathbf{i}}$ to find:

$$\begin{aligned}
\ddot{\hat{x}} - 2\dot{\hat{y}} &= 3\hat{x} - \frac{1}{\chi^3}\sum_{k=-\infty}^{\infty} \frac{\hat{x}}{\left[\hat{x}^2 + \left(\frac{2k}{\chi\sigma^{1/3}} - \hat{y}\right)^2 + \hat{z}^2\right]^{3/2}} \\
\ddot{\hat{y}} + 2\dot{\hat{x}} &= -\frac{1}{\chi^3}\sum_{k=-\infty}^{\infty} \frac{\hat{y} - \frac{2k}{\chi\sigma^{1/3}}}{\left[\hat{x}^2 + \left(\frac{2k}{\chi\sigma^{1/3}} - \hat{y}\right)^2 + \hat{z}^2\right]^{3/2}} \\
\ddot{\hat{z}} &= -\hat{z} - \frac{1}{\chi^3}\sum_{k=-\infty}^{\infty} \frac{\hat{z}}{\left[\hat{x}^2 + \left(\frac{2k}{\chi\sigma^{1/3}} - \hat{y}\right)^2 + \hat{z}^2\right]^{3/2}}.
\end{aligned} \tag{37}$$

In this approximation the ring becomes a straight line of equally spaced particles. See Figure 2 for a representation of the geometry in these equations of motion.

The coordinates of the particles are $(\hat{x}_k = 0, \hat{y}_k = \frac{2k}{\chi\sigma^{1/3}}, \hat{z}_k = 0)$, $k = 0, \pm 1, \pm 2, \ldots$. The distance between each particle is $\frac{2}{\chi\sigma^{1/3}}$.

It is desirable to find a potential function for the forms in this system. If such a potential can be found, then an energy integral exists as the system is time invariant. Formally integrate the following partial differential equations:

$$\begin{aligned}
\hat{V}_{\hat{x}} &= 3\hat{x} + F_{\hat{x}} \\
\hat{V}_{\hat{y}} &= F_{\hat{y}} \\
\hat{V}_{\hat{z}} &= -\hat{z} + F_{\hat{z}}.
\end{aligned} \tag{38}$$

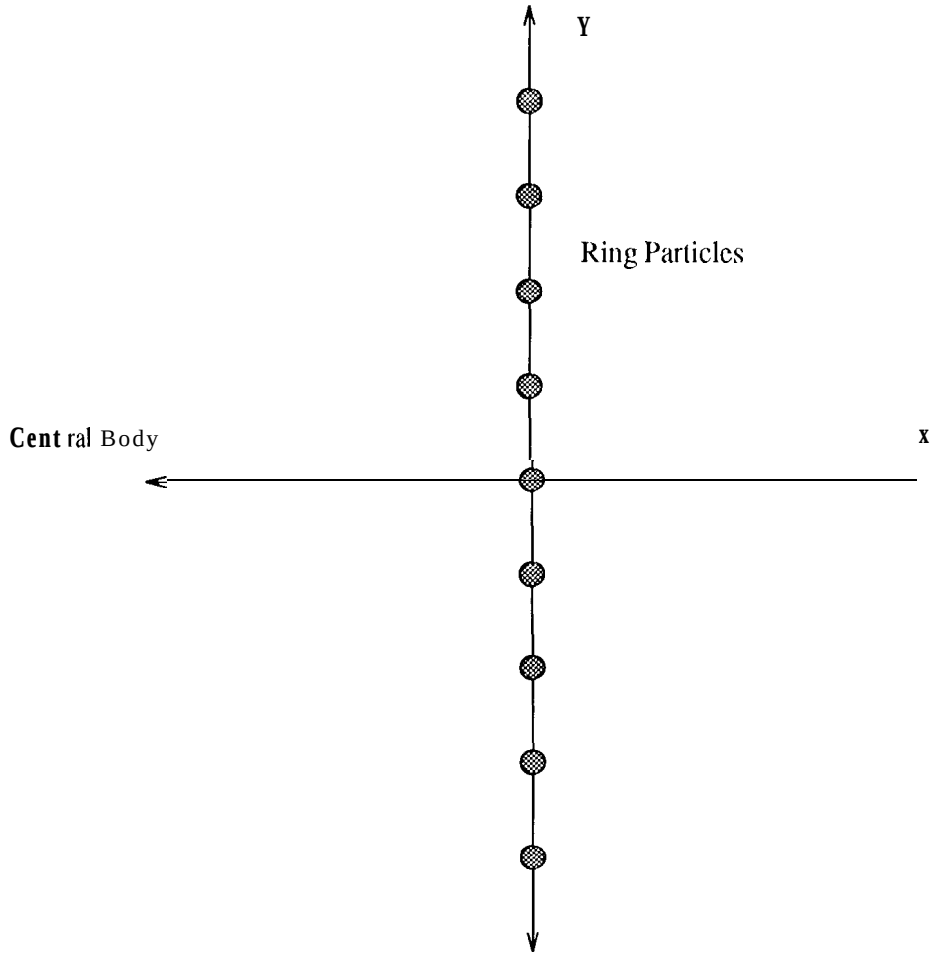

Figure 2: Geometrical Representation of the Close Ring Approximation

This yields a potential of the form:

$$\hat{V}(\hat{x},\hat{y},\hat{z}) = \frac{3}{2}\hat{x}^2 - \frac{1}{2}\hat{z}^2 + \frac{1}{\chi^3}\sum_{k=-\infty}^{\infty}\frac{1}{\sqrt{\hat{x}^2 + \left(\frac{2k}{\chi\sigma^{1/3}} - \hat{y}\right)^2 + \hat{z}^2}} - \hat{C}. \tag{39}$$

This summation is not defined as it is asymptotically equivalent to the summation $\sum_{k=1}^{\infty} 1/k$ which diverges. Note that the partials of $\hat{V}$ are convergent series and hence the divergent part of $\hat{V}$ may be considered to be constant. This leads to a a particular choice of the constant $\hat{C}$ to kill the divergent terms, yielding the potential:

$$\hat{V}(\hat{x},\hat{y},\hat{z}) = \frac{3}{2}\hat{x}^2 - \frac{1}{2}\hat{z}^2 + \frac{1}{\chi^3}\frac{1}{\sqrt{\hat{x}^2+\hat{y}^2+\hat{z}^2}} + \frac{1}{\chi^3}\sum_{k=-\infty}^{\infty}{}' \left| \frac{1}{\sqrt{\hat{x}^2 + \left(\frac{2k}{\chi\sigma^{1/3}} - \hat{y}\right)^2 + \hat{z}^2}} - \frac{\chi\sigma^{1/3}}{2|k|} \right|. \tag{40}$$

As can be verified, this summation is convergent for all non-singular values of the coordinates.

With this potential the energy integral is defined as:

$$\frac{1}{2}\left(\dot{\hat{x}}^2+\dot{\hat{y}}^2+\dot{\hat{z}}^2\right) = \hat{V}(\hat{x},\hat{y},\hat{z})-\hat{C} \tag{41}$$

where $\hat{C}$ is a finite constant.

5.1 Modified Hill Equations of Motion

Now consider the arbitrary scale factor χ. Two possible values for this factor are considered which lead to two different sets of equations of motion. First consider the equations for $\chi = 1$. Retain the tilde notation for this case. The equations of motion become:

$$\begin{aligned}\ddot{\hat{x}}-2\dot{\hat{y}} &= \hat{V}_{\hat{x}}\\ \ddot{\hat{y}}+2\dot{\hat{x}} &= \hat{V}_{\hat{y}}\\ \ddot{\hat{z}} &= \hat{V}_{\hat{z}}\end{aligned} \tag{42}$$

$$\begin{aligned}\hat{V}(\hat{x},\hat{y},\hat{z}) = {} & \frac{3}{2}\hat{x}^2-\frac{1}{2}\hat{z}^2+\frac{1}{\sqrt{\hat{x}^2+\hat{y}^2+\hat{z}^2}}\\ & +\sum_{k=-\infty}^{\infty}{}'\left[\frac{1}{\sqrt{\hat{x}^2+\left(\frac{2k}{\sigma^{1/3}}-\hat{y}\right)^2+\hat{z}^2}}-\frac{\sigma^{1/3}}{2|k|}\right].\end{aligned} \tag{43}$$

In these coordinates the ring particles are separated by a distance $2/\sigma^{1/3}$. Thus, if σ is small, the distance between ring particles becomes large. This system is useful in discussing the dynamics of a body close to a ring particle, but not directly interacting with neighboring ring particles. If $\sigma \to 0$ the Hill equations of motion are recovered. Due to this property this system is called the "Modified Hill" equations of motion.

5.2 Close Ring Equations of Motion

A second possibility for the scale factor is $\chi = 1/\sigma^{1/3}$. Denote the coordinates in this case as x, y and z. These new coordinates are related to the previous coordinates by the transformations:

$$\begin{aligned}\hat{x} &= \frac{1}{\sigma^{1/3}}x\\ \hat{y} &= \frac{1}{\sigma^{1/3}}y\\ \hat{z} &= \frac{1}{\sigma^{1/3}}z\end{aligned} \tag{44}$$

These transformations become singular as $\sigma \to 0$, yet from the derivation of the equations of motion the approximation process is valid for all σ when $\chi = 1/\sigma^{1/3}$, since the higher order terms in Equation 21 are then $\mathcal{O}(\theta)$ and still go to zero under the limit.

For this value of χ the equations of motion become:

$$\begin{aligned}\ddot{x}-2\dot{y} &= V_x\\ \ddot{y}+2\dot{x} &= V_y\\ \ddot{z} &= V_z\end{aligned} \tag{45}$$

$$V(x,y,z) = \frac{3}{2}x^2 - \frac{1}{2}z^2 + \frac{\sigma}{\sqrt{x^2+y^2+z^2}} + \sigma \sum_{k=-\infty}^{\infty}{}' \left[\frac{1}{\sqrt{x^2+(2k-y)^2+z^2}} - \frac{1}{2|k|} \right]. \quad (46)$$

Then energy integral becomes:

$$\frac{1}{2}\left(\dot{x}^2+\dot{y}^2+\dot{z}^2\right) = V(x,y,z) - C \quad (47)$$

In these coordinates the spacing between ring particles is now a constant distance 2 and does not depend on σ. Due to this property these equations of motion are more efficient for studying the orbit of a particle which may travel from ring particle to ring particle. If $\sigma \to 0$ a simple set of integrable equations is recovered corresponding to linearized motion about a circular orbit,.

These equations are called the "Close Ring" equations of motion. In the following sections the basic properties of the equations of motion 42 and 45 are studied.

6 Invariant Transformations

The following discussion deals only with the Close Ring equations of motion (Equations 45), although all the results are easily carried over to the modified Hill equat ions of motion (Equations 42).

Equations 45 arc invariant under several different transformations. These transformations highlight the structure in the equations and allow for simplifications to be introduced,

The z equation of motion is invariant under two separate transformations:

$$(z,\tau) \to (-z,\tau) \quad (48)$$

$$(z,\tau) + (2,-\mathrm{T}). \quad (49)$$

The first transformation may always be applied to any given three-dimensional solution, yielding a mirror image motion in the $-z$ space. The second may only be applied in conjunction with the invariant time reversal transformation in the (x, y, τ) space discussed later. The following discussion only considers the (x,y) coordinates.

The simplest invariant transformation the equations posses (other than time invariant.c) is:

$$(3', y, \tau) \to (x, y+2k, \tau) \quad (50)$$

$$k = 0, \pm 1, \pm 2, \ldots$$

The geometry of the problem does not change under this transformation.

A second invariant, transformation is:

$$(x, y, \tau) \to (x, -y, -\tau). \quad (51)$$

This is a space-time symmetry transformation. This transformation, in conjunction with the previous transformation, is useful in establishing the existence of symmetric periodic orbits.

A final invariant transformation is:

$$(x, y, \tau) \to (-r, -y, T). \quad (52)$$

This is a space symmetry transformation. Additional invariant transformations exist, but arc not needed in the ensuing discussion.

The invariant transformations are useful in establishing the existence of space symmetric motions. In this Context consider the initial conditions and time under the invariant, transformations:

$$(x_o, y_o, \dot{x}_o, \dot{y}_o, \tau) \rightarrow (x_o, y_o + 2k, \dot{x}_o, \dot{y}_o, \tau) \tag{53}$$
$$k = 0, \pm 1, \pm 2, \ldots$$
$$(x_o, y_o, \dot{x}_o, \dot{y}_o, \tau) \rightarrow (x_o, -y_o, -\dot{x}_o, \dot{y}_o, -\tau) \tag{54}$$
$$(x_o, y_o, \dot{x}_o, \dot{y}_o, \tau) \rightarrow (-x_o, -y_o, -\dot{x}_o, -\dot{y}_o, \tau). \tag{55}$$

If some set of initial conditions transforms into itself, then the motion starting from these initial conditions will have a special space symmetry property. Several special properties are considered below.

Transformation 53 by itself results in a reduction of the y-coordinate space to the strip $(-1, 1]$, Used in conjunction with the other transformations it proves quite useful.

Transformation 54 will transform into itself if $y_o = \dot{x}_o = 0$. Due to the time reversal this implies that the initial conditions $(x_o, 0, 0, \dot{y}_o)$ lead to a space symmetric motion with respect to the $y_o = 0$ axis. Combining transformation 53 with transformation 54, the initial conditions $(x_o, k, 0, \dot{y}_o), k = 0, +1, +2, \ldots$ lead to space symmetric orbits about $y_o = k$.

Transformation 55 is useful in two ways. Given any motion started in the $x_o > 0$ region of the space, a companion motion starting in the $x_o < 0$ region of the spat.c may be inferred. Furthermore, if a discrete set of initial conditions are found which can be transformed into themselves, then these initial conditions arc an equilibrium point of the system. This is so as the time is not reversed in this transformation and hence the motion must remain space symmetric to itself for all time, a property shared only by an equilibrium point. The only initial condition which transforms to itself under the action of this transformation alone is the trivial set (0, 0, 0, 0), which is discounted due to the singularity at, these coordinates. If Transformation 55 is combined with Transformation 53 the initial conditions $(0, 2k + 1, 0, 0), k = 0, +1, \pm 2, \ldots$ will transform into themselves and arc not located at singularities. Thus, these points are equilibrium points and lie midway between each ring particle on the $x = 0$ axis. These equilibrium points arc discussed in following sections.

The invariant transformations also allow the coordinate space to be restricted to:

$$\begin{aligned} 0 \leq x &< \infty \\ -1 < y &\leq 1 \\ 0 \leq z &< \infty. \end{aligned} \tag{56}$$

Generally only the initial conditions arc restricted to this space. 'I'lien the resultant motion is allowed to travel over the whole space.

7 Modified Hill Equations of Motion

Some basic properties, results and uses for these equations are noted. The equations arc restated as:

$$\begin{aligned} \ddot{\hat{x}} - 2\dot{\hat{y}} &= \tilde{V}_{\hat{x}} \\ \ddot{\hat{y}} + 2\dot{\hat{x}} &= \tilde{V}_{\hat{y}} \\ \ddot{\hat{z}} &= \tilde{V}_{\hat{z}} \end{aligned} \tag{57}$$

where the potential is:

$$\tilde{V}(\hat{x}, \hat{y}, \hat{z}) = \frac{3}{2}\hat{x}^2 - \frac{1}{2}\hat{z}^2 + \frac{1}{\sqrt{\hat{x}^2 + \hat{y}^2 + \hat{z}^2}}$$

$$+\sigma^{1/3}\sum_{k=-\infty}^{\infty}{}' \left[\frac{1}{\sqrt{\sigma^{2/3}\hat{x}^2+\left(2k-\sigma^{1/3}\hat{y}\right)^2+\sigma^{2/3}\hat{z}^2}}-\frac{1}{2|k|}\right] \tag{58}$$

These equations are most interesting for small cr. Expand the potential in orders of $\sigma^{1/3}$ to find:

$$\begin{aligned}\hat{V}(\hat{x},\hat{y},\hat{z}) = {} & \frac{1}{2}\left[3-\frac{1}{4}\sigma\zeta(3)\right]\hat{x}^2-\frac{1}{2}\left[1+\frac{1}{4}\sigma\zeta(3)\right]\hat{z}^2+\frac{1}{4}\sigma\zeta(3)\hat{y}^2 \\ & +\frac{1}{\sqrt{\hat{x}^2+\hat{y}^2+\hat{z}^2}}+\mathcal{O}(\sigma^{4/3}).\end{aligned} \tag{59}$$

The function $\zeta(3)=\sum_{k=1}^{\infty}1/k^3=1.20205\ldots$. Truncate the higher order terms in the potential to find the approximate equations of motion:

$$\begin{aligned}\ddot{\hat{x}}-2\dot{\hat{y}} &= \left[3-\frac{1}{4}\sigma\zeta(3)\right]\hat{x}-\frac{\hat{x}}{\left[\hat{x}^2+\hat{y}^2+\hat{z}^2\right]^{3/2}} \\ \ddot{\hat{y}}+2\dot{\hat{x}} &= \frac{1}{2}\sigma\zeta(3)\hat{y}-\frac{\hat{y}}{\left[\hat{x}^2+\hat{y}^2+\hat{z}^2\right]^{3/2}} \\ \ddot{\hat{z}} &= -\left[1+\frac{1}{4}\sigma\zeta(3)\right]\hat{z}-\frac{\hat{z}}{\left[\hat{x}^2+\hat{y}^2+\hat{z}^2\right]^{3/2}}.\end{aligned} \tag{60}$$

These equations arc valid for small σ only. It is directly apparent that the Hill equations of motion arc recovered as a $\rightarrow$ O.

This system, under the coordinate restrictions given in Equations 56, has several equilibrium points, some of which are not present in the Classical hill equations of motion. Take $\hat{z}=$ O to fine] the two conditions to be met for an equilibrium point to exist:

$$0 = \left(3-\frac{1}{4}\sigma\zeta(3)-\frac{1}{\left[\hat{x}^2+\hat{y}^2\right]^{3/2}}\right)\hat{x} \tag{61}$$

$$0 = \left(\frac{1}{2}\sigma\zeta(3)-\frac{1}{\left[\hat{x}^2+\hat{y}^2\right]^{3/2}}\right)\hat{y}. \tag{62}$$

There are three possibilities to investigate: ($\hat{x}\neq$ O, $\hat{y}=$ O), ($\hat{x}=$ O, $\hat{y}\neq$ O) and ($\hat{x}\neq$ O, $\hat{y}\neq$ O). Each is considered in turn.

First consider the case when $\hat{y}$ = O and $\hat{x}\neq$ O. Then the conditions 61 and 62 reduce to:

$$0 = 3-\frac{1}{4}\sigma\zeta(3)-\frac{1}{|\hat{x}|^3}. \tag{63}$$

Take $\hat{x}>0$ to find the equilibrium point denoted E1 with coordinate:

$$\hat{x}_1 = \left(\frac{1}{3}\right)^{1/3}\left[1-\frac{1}{12}\sigma\zeta(3)\right]^{-1/3} \tag{64}$$

$$\approx \left(\frac{1}{3}\right)^{1/3}\left[1+\frac{1}{36}\sigma\zeta(3)\right]. \tag{65}$$

There is a corresponding equilibrium point, denoted E2, with coordinate $\hat{x}_2=-\hat{x}_1$. These equilibrium points are the generalization of the equilibrium points in the Hill equations of motion. They arc saddle points and hence are unstable.

Next consider the case $\hat{x}$ = O, $\hat{y}\neq$ O. Then the conditions reduce to:

$$0 = \frac{1}{2}\sigma\zeta(3)-\frac{1}{|\hat{y}|^3}. \tag{66}$$

Take $\tilde{y} > 0$ to find the equilibrium point denoted $E3$ with coordinate:

$$\begin{aligned} \tilde{y}_3 &= \left(\frac{2}{\sigma\zeta(3)}\right)^{1/3} \\ &\approx \frac{1.185\ldots}{\sigma^{1/3}}, \end{aligned} \tag{67}$$

For σ small this equilibrium point is far away from the origin. This equilibrium point is more properly discussed using the Close Ring equations of motion in Section 8.

Finally consider the case when $\tilde{x} \neq 0$ and $y \neq 0$. Then the conditions reduce to:

$$0 = 3 - \frac{1}{4}\sigma\zeta(3) - \frac{1}{|\tilde{r}|^3} \tag{68}$$

$$0 = \frac{1}{2}\sigma\zeta(3) - \frac{1}{|\tilde{r}|^3} \tag{69}$$

where $\tilde{r} = \sqrt{\tilde{x}^2 + \tilde{y}^2}$.

These conditions are satisfied only if

$$\begin{aligned} \sigma &= \frac{4}{\zeta(3)} \\ &\approx 3.327\ldots \end{aligned} \tag{70}$$

$$\begin{aligned} \tilde{r} &= \left(\frac{1}{2}\right)^{1/3} \\ &\approx 0.794\ldots. \end{aligned} \tag{71}$$

This is outside the realm of applicability for the approximation made in deriving these equations of motion, and this point does not exist in Equations 57. This possibility is only mentioned since at this value of σ Equations 60 are integrable due to the existence of au angular momentum integral. This may be of mathematical interest as it provides a modification to the Hill equations which results in an integrable system.

A prime application of Equations 60 would be to any analysis which traditionally uses the Hill equations to model ring or asteroid dynamics. '1'here are a number of such studies and it would be of interest to recompute results using these modified equations ([1], [2], [4], [5], [6], [1 1], [17]). The current model includes the effect of neighboring particles, parameterized by u, on the dynamics of a small particle when a close encounter with a ring particle occurs. These equations might also be applicable to the study of shepherding in which the classical hill equations of motion are often used. They have a natural "boundary condition)' as they provide a finite value of the $\tilde{y}$ coordinate at which there is a space symmetry. III usual shepherding studies using the Hill equations the interaction must be carried to $\tilde{y} = \pm\infty$.

In performing such new analyses it is possible to first consider the results found in the traditional Hill equations and then consider the modification of these results as σ increases from O. A prime application of this type of analysis would be to generalize the Variation orbit in the Hill equations.

The Variation orbit is an analytical periodic solution of the Hill equations ([19], Chapter VI, $503-51 5). It is expressed in the form of a Fourier series to any desired accuracy. It is possible to generalize the analytic form of the solution to include the parameter σ and its effects, thus finding a periodic orbit in the modified Hill equations by analytic continuation. No qualitative differences arise from this change for σ small. We do not explicitly state our results of this analysis here.

8 Close Ring Equations of Motion

Now consider the Close Ring equations of motion. These are restated as:

$$\begin{aligned} \ddot{x} - 2\dot{y} &= V_x \\ \ddot{y} + 2\dot{x} &= V_y \\ \ddot{z} &= V_z \end{aligned} \tag{72}$$

$$V(x,y,z) = \frac{3}{2}x^2 - \frac{1}{2}z^2 + \frac{\sigma}{\sqrt{x^2+y^2+z^2}} + \sigma \sum_{k=-\infty}^{\infty}{}' \left[\frac{1}{\sqrt{x^2+(2k-y)^2+z^2}} - \frac{1}{2|k|} \right] \tag{73}$$

These equations are more novel than the previous set in that they allow for the simple description of orbits which travel from one ring part, icle to another.

These equations allow simple analytic solutions in very few cases and thus it is preferable to study them numerically. This task is simplified as there is only one parameter in the equations, σ. Note, however, that the infinite summations in the potential and force terms can only be computed to a finite accuracy and prove to be the most time consuming aspect of the computation.

Again, consider the equilibrium points of this system. First take z = O to find the conditions for equilibrium points to exist:

$$0 = 3 - \sigma \sum_{k=-\infty}^{\infty} \left[\frac{1}{|x|^3} + \frac{1}{[(2k-y)^2]^{3/2}} \right] \tag{74}$$

$$0 = -\sigma \sum_{k=-\infty}^{\infty} \frac{y-2k}{[x^2+(2k-y)^2]^{3/2}} \tag{75}$$

The expression 75 is identically zero only for y = O, ±1, ±2, ... There are two distinct cases to consider: y = O and y = 1.

Take y = O and $x \geq$ O. Assume $x \neq$ O to avoid the singularity. Condition 74 becomes:

$$0 = 3 - \sigma \sum_{k=-\infty}^{\infty} \frac{1}{[x^2+(2k)^2]^{3/2}}. \tag{76}$$

If x <<1 and σ >0 the quantity on the right hand side will be negative (clue to the k = O term). Conversely, if x >> 1 and $\sigma < \infty$ the quantity will be positive. Thus there is at least one equilibrium point along the x axis. In analogy with the Modified Hill equations call this equilibrium point E]. Borrowing the result, from the Modified Hill equations the coordinate of this equilibrium point is, approximately:

$$x_1 \approx \left(\frac{\sigma}{3}\right)^{1/3} \left[1 + \frac{\sigma}{36}\zeta(3) + \cdots\right] \tag{77}$$

There is a corresponding equilibrium point E2 located at $x_2 = -x_1$ Note that as $\sigma \to 0$ in this system the $E1$ equilibrium point moves into the origin. Contrast this with the El equilibrium point in the Modified Hill equations (Equation 64) where the equilibrium point moves toward a fixed, Hol]-zero coordinate as σ decreases. This highlights the difference between these two dynamical systems.

That there is only one equilibrium point along the positive x axis is established as follows. Let x^* be an equilibrium point, then for all $x > x^*$ the inequality holds:

$$3 - \sigma \sum_{k=-\infty}^{\infty} \frac{1}{[x^2+(2k)^2]^{3/2}} > 3 - u \sum_{k=-\infty}^{\infty} \frac{1}{[(X^*)23-(2k)^2]^{3/2}} = 0. \tag{78}$$

Thus, if x^* is an equilibrium point, there are no equilibrium points $> x^*$. Combine this with the fact that there is at least one equilibrium point on the axis to conclude that there is only one equilibrium point on the positive x axis.

As in the previous cases, these equilibrium points are saddle points and hence are unstable

Next consider $y = 1$ and $x \geq 0$. Condition 75 becomes:

$$0 = 3 - \sigma \sum_{k=-\infty}^{\infty} \frac{1}{[x^2 + (2k-1)^2]^{3/2}} x. \tag{79}$$

Note that $x = 0$ will satisfy the condition for all σ. This is the equilibrium point found by the symmetry transformation analysis and corresponds to the equilibrium point briefly discussed in the Modified Hill equations (Equation 67). If σ is sufficiently small, this will be the only equilibrium point,. If σ is large enough, there will be additional equilibrium points along the $y = 1$ axis.

First consider the $x = 0$ equilibrium point and its stability. Computing the second partials of the potential function evaluated at the equilibrium point yields:

$$V_{xx}|_o = 3 - \frac{7}{4}\sigma\zeta(3) \tag{80}$$

$$V_{yy}|_o = \frac{7}{2}\sigma\zeta(3). \tag{81}$$

$V_{yy}|_o$ is always positive but $V_{xx}|_o$ is positive only for $\sigma < 12/7\zeta(3)$. The sign change in $V_{xx}|_o$ corresponds to a bifurcation of new equilibrium points and is discussed shortly.

Thus, for σ small enough the equilibrium point is a local minimum of the potential and may be stable. The characteristic equation for assumed harmonic motion in the vicinity of the equilibrium point is:

$$\lambda^4 + \left[1 - \frac{7}{4}\sigma\zeta(3)\right]\frac{7}{4}\sigma\zeta(3)\lambda^2 + \frac{7}{2}\sigma\zeta(3)\left[3 - \frac{7}{4}\sigma\zeta(3)\right] = 0. \tag{82}$$

The controlling stability condition is then:

$$\frac{441}{16}\sigma^2\zeta(3)^2 - \frac{91}{2}\sigma\zeta(3) + 1 > 0\ . \tag{83}$$

This leads to a bound on σ for stability:

$$\sigma < \sigma_{E_3} \tag{84}$$

$$\sigma_{E_3} = \frac{4}{7\zeta(3)}\frac{1}{13 + 4\sqrt{10}} \tag{85}$$

$$= \frac{1}{4}\sigma_S$$

$$\approx 0.01853. .$$

Note that this is exactly 1/4 the value of the stability bound on the ring. This result also corresponds with the asymptotic result found when the number of ring particles P is finite, but large (Reference [14]). The implications of the existence of this stable equilibrium point are discussed later. The energy parameter C takes on a special value at these equilibrium points:

$$C_{E_3} = \sigma(1 + 2\ln 2) \tag{86}$$

$$= 2.386 \ldots \sigma$$

Now consider the possibility of other equilibrium points along the $y = 1$ axis. The condition to satisfy in this case is:

$$0 = 3 - \sigma \sum_{k=-\infty}^{\infty} \frac{1}{[x^2 + (2k-1)^2]^{3/2}} \tag{87}$$

This condition may be satisfied if and only if $\sigma \geq 12/7((3) = 1 .426....$ Again, if there is an equilibrium point for $x > 0$, then it is unique.

As noted before, for $\sigma > 12/7<(3)$ the $x = O$ equilibrium point becomes a saddle point. The $x > 0$ equilibrium point, is then a local minimum of the potential function. The stability of these points are not studied, however, as they correspond to an unstable ring $(u > \sigma s)$.

9 A Family of Periodic Orbits

A special family of periodic orbits are now studied using the Close Ring equations of motion (Equations 72). This family consists of planar orbits symmetric about the $y = O$ and $y = 1$ axis. This family shows some remarkable properties which may inspire the study of this system. Unfortunately the family cannot currently be traced to termination due to accuracy and modeling constraints. See Figure 3 for some representative periodic orbits for a specific value of σ. Note that some of the members of this family encircle the E3 equilibrium point

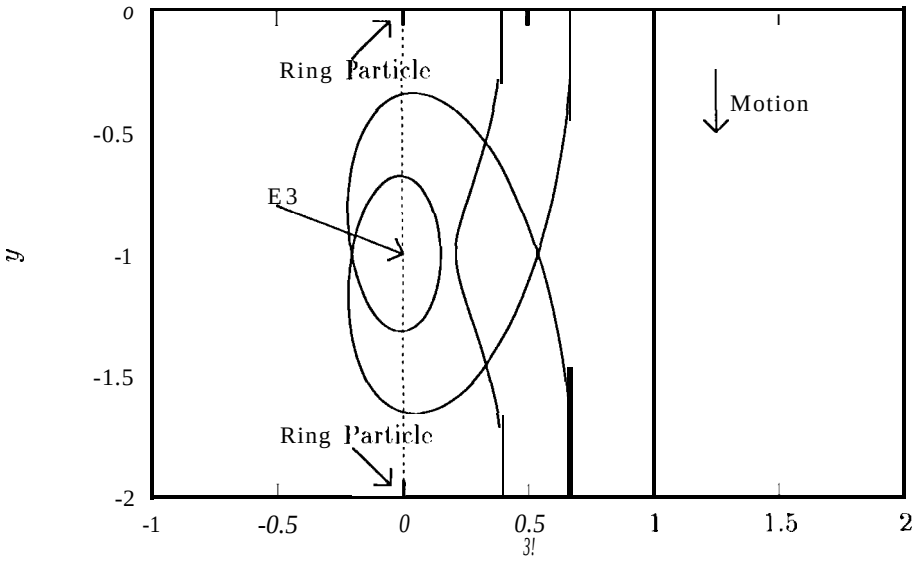

Figure 3: Symmetric Periodic orbits: $\sigma = \sigma_{E_3}$

The family of orbits discussed in this section are all found numerically. The special form of the initial conditions for space-symmetric orbits ($\dot{x}_o = y_o = O$) reduce the initial conditions to the pair $x_o, \dot{y}_o$. The energy integral may be used to remove one of these conditions. Thus there are three parameters to be varied to find a periodic orbit: x_o, C, σ. A specific family of periodic orbits describes a surface in this three-dimensional parameter space. For this discussion the parameter σ is fixed and the parameters x_o and C are computed for a particular family. The family then describes a curve in this two-dimensional parameter space. These curves are computed for several values of σ.

The planar and out-of-plane monodromy matrices are also computed for these families to determine the stability of the orbits. Additionally, the possibility of intersection of this family of periodic orbits with other families is considered. Some of the following theoretical discussion (Section 9.1 - 9.4) is borrowed from Hénon's elegant analysis [3]. The results are briefly restated as they are being applied to a set of equations not dealt with previously in the literature.

9. I Reduction of the Equations of Motion

When dealing with numerical solutions to the equations of motion it is possible to introduce theoretical reductions to the equations which are not feasible analytically, Two such reductions are applied to the dynamical system.

First consider the energy integral. Formally, the integral allows for the elimination of one variable from consideration. Thus, conceptually, motion in the dynamical system may be described by three variables plus a specified value of energy, C. Assume that the variable $\dot{y}$ is eliminated via the energy integral. Then the system is described by the three variables x, y and $\dot{x}$ and the energy parameter C. Given initial conditions, these solutions are specified as:

$$x(t) = h_1(x_o, y_o, \dot{x}_o, C; t) \tag{88}$$

$$y(t) = h_2(x_o, y_o, \dot{x}_o, C; t) \tag{89}$$

$$\dot{x}(t) = h_3(x_o, y_o, \dot{x}_o, C; t). \tag{90}$$

of interest are the special initial conditions which start at y_o = O and at some later time cross the value of y defined as $y_k = k; k = 0, \pm 1, \pm 2, \ldots$.

Under some mild restrictions a second reduction may be introduced, this reduction being the Poincaré Map. A Poincaré Map is constructed by finding two surfaces in the phase space which the solution is transverse to. Then the solution between intersections with these surfaces is disregarded (assuming it is continuous and smooth) and one only considers the mapping of the solution from one surface to the other.

In this system the natural candidate surfaces are y_o and y_k. The transversality conditions are then $\dot{y}_o \neq$ O and $\dot{y}_k \neq$ O. For the orbits considered, $\dot{y}_o$ # O is always fulfilled by choice. In some instances $\dot{y}_k =$ O occurs, but another value of k may always be chosen to reintroduce the proper transversality condition.

Under the Poincaré Map, the dynamical system is reduced to two non-linear maps:

$$x_k = f(x_o, \dot{x}_o, C) \tag{91}$$

$$\dot{x}_k = g(x_o, \dot{x}_o, \mathbf{C}). \tag{92}$$

Simple analytical forms for these maps are known only in the trivial case when $\sigma =$ O. The maps are usually computed by numerical integration of the equations of motion.

9,2 Computation of Periodic Orbits

With the above reduced system, the necessary aud sufficient conditions for a space-symmetric periodic orbit to exist, arc (see Reference [16], Section 4 .52):

$$\dot{x}_o = o \tag{93}$$

$$\dot{x}_k = 0. \tag{94}$$

If k is even and $x_k = x_o$ the conditions may be simplified to:

$$\dot{x}_o = o \tag{95}$$

$$\dot{x}_{k/2} = o. \tag{96}$$

Thus given $\sigma, \dot{x}_o$ = O, and a final surface of section y_k, there is only one condition to be met to determine a symmetric periodic orbit:

$$g(x_o, 0, C) = o . \tag{97}$$

An update scheme may be derived from this equation which leads to convergence on a periodic orbit if initially close to a periodic. orbit.

Assume that x_o and C are close to, but do not fulfill, Condition 97. Assume they arc modified by dx_o and dC so that the condition is fulfilled. Using a truncated Taylor series expansion yields the equation to be satisfied:

$$g(x_o, 0, \text{c}) + g_x|_o dx + \text{g(,.lode} = o\ . \tag{98}$$

In the above, the notation $g_x|_o$ denotes the partial of g with respect to x and $g_C|_o$ denotes the partial of g with respect to C, all evaluated at the nominal conditions $x_o, \dot{x}_o$ and C. Generally, both partials of g will not be zero sim ultaneously. Thus there arc two update schemes available:

$$dC = -\frac{g(x_o, 0, C)}{g_C|_o} \tag{99}$$

$$dx = -\frac{g(x_o, 0, C)}{g_x|_o}\ \text{“} \tag{loo}$$

Repeated correction with these update schemes will lead to convergence on a periodic orbit in most cases. The partials of g may be inferred from the state transition matrix of the variational equations integrated along the nominal orbit. in practice there may be points where one of the partials is zero. In these cases the other update scheme may be used.

9.3 Stability Analysis of Symmetric Orbits

Once a periodic. orbit has been found it is of interest to determine the stability of the orbit in both the in-plane and out-of-plane directions.

9.3.1 In-Plane Stability

Consider the cqui-energy variation of the variables x_o and $\dot{x}_o$ about the fixed points of the previous maps 91 and 92. Assume that the maps arc evaluated over one full period of tile orbit. The equations of variation arc:

$$\begin{bmatrix} dx_k \\ d\dot{x}_k \end{bmatrix} = \begin{bmatrix} f_x & f_{\dot{x}} \\ g_x & g_{\dot{x}} \end{bmatrix} \begin{bmatrix} dx_o \\ d\dot{x}_o \end{bmatrix} \tag{101}$$

In the above, the partials f_x, etc., are evaluated at the initial conditions for the periodic orbit. They are solved for from the state transition matrix of the variation equations integrated along the periodic orbit. Note that $f_x = g_{\dot{x}}$, a genera] property for symmetric planar orbits. Also note that $f_x^2 - f_{\dot{x}} g_x = 1$ duc to volume conservation in phase space.

Thus the dynamics of an orbit perturbed from a space-symmetric periodic orbit arc described by the linear mapping:

$$\begin{bmatrix} dx_k \\ d\dot{x}_k \end{bmatrix} = \begin{bmatrix} f_x & f_{\dot{x}} \\ g_x & f_x \end{bmatrix} \begin{bmatrix} dx_o \\ d\dot{x}_o \end{bmatrix}. \tag{102}$$

The linear stability of the orbit is determined by the eigenvalues of this matrix, computed from the polynom ial:

$$\lambda^2 - 2f_x\lambda + 1 = 0. \tag{103}$$

For stability, both roots to this equation must have unit magnitude, i.e. $|\lambda| = 1$. This result occurs if and only if

$$-1 \leq f_x \leq 1.. \tag{104}$$

‘1’0 evaluate the planar stability of an orbit, one need only determine the value f_x. For a space-symmetric orbit the value k will be even and stability may be determined from the linear mapping of y_o to $y_{k/2}$ as detailed in Reference [7], Section 10.7.4.3.

The stability of the orbit changes when f_x passes through the values ± 1. As will be seen, at these critical values the family of periodic. orbits may intersect with another family of periodic orbits.

9.3.2 Out-of-Plane Stability

Once the periodic orbit has been found the out-of-plane variation equation is fouud to be:

$$\ddot{z} = V_{zz}|_o z \tag{105}$$

where $V_{zz}|_o$ is a time-varying periodic matrix. In state space form the variation equations arc:

$$\begin{bmatrix} \dot{z} \\ \ddot{z} \end{bmatrix} = \begin{bmatrix} \text{A m} \end{bmatrix} \tag{106}$$

Given the trajectory of the periodic orbit, this linear equation may be integrated numerically to find the state transition matrix from y_o to y_k (the monodromy matrix). Again, the orbit, is out-of-plane stable if the eigenvalues of the monodromy matrix have modulus 1.

9.4 Local Continuation of the Symmetric Family

Having found one periodic orbit, it is possible to compute other members of the same family. Wc do not consider continuation in the σ parameter, although this could be done. We only consider continuation in the (x_o, C) plane and possible intersection with symmetric and non-symmetric families of periodic orbits.

Consider the fixed point of the space symmetric periodic orbit:

$$x_o = f(x_o, o, c) \tag{107}$$

$$o = g(x_o, 0, c). \tag{108}$$

To continue the family the tangent to the family at this point must be found. The tangent will satisfy the equations:

$$dx_o = f_x dx_o + f_{\dot{x}} d\dot{x}_o + f_C\, dC \tag{109}$$

$$d\dot{x}_o = g_x dx_o + f_x d\dot{x}_o + g_C dC. \tag{110}$$

Note that $f_x = g_{\dot{x}}$ as before. Also, from the space-symmetric properties of the orbit, the tangent equations should be invariant under a sign change of $d\dot{x}_o$. This decouples the tangent equations as:

$$\begin{bmatrix} f_x - 1 & f_C \\ g_x & g_C \end{bmatrix} \begin{bmatrix} dx_o \\ dC \end{bmatrix} = \begin{bmatrix} 0 \\ 0 \end{bmatrix} \tag{111}$$

$$\begin{bmatrix} f_{\dot{x}} & f_x - 1 \end{bmatrix} d\dot{x}_o = \begin{bmatrix} 0 & 0 \end{bmatrix} \tag{112}$$

Recall the volume conservation relation

$$f_x^2 - f_{\dot{x}} g_x = 1 \tag{113}$$

Note that the first tangent equation must be singular for a non-zero tangent to exist, in the dx_o, dC plane. This equation is indeed singular, thus the additional relation:

$$g_C(f_x - 1) - f_C g_x = o. \tag{114}$$

The tangent to the family will reside in the null space of the above equations 111 aud 112.

There are three different cases to consider: $f_x \neq 1$, $f_x = 1$, $f_x = -1$.

9.4.1 $f_x + 1$

There are a number of implications which may be lain out immediately:

$$f_{\dot{x}} \neq 0 \tag{115}$$

$$g_x \neq 0 \tag{116}$$

$$\frac{g_C}{g_x} = \frac{f_C}{f_x - 1}. \tag{117}$$

First note that $d\dot{x}_o$ = O as its coefficients are non-zero. Thus, in this case, the family will not intersect a non-symmetric family of the same period.

The tangents to the current family are,:

$$dx_o = -\frac{f_C}{f_x - 1} dC \tag{118}$$

$$dx_o = -\frac{g_C}{g_x} dC. \tag{119}$$

These two tangents are equivalent due to Relation 117. 'J'bus, a tangent always exists in this case and defines the local evolution of the family. If f_C = O then g_C = O and dx_o = *O,* but dC is free to vary. In this case, the tangent to the family is parallel to the C parameter and is normal to the x_o variable, i.e. the family is at a local extremum with respect, to the x_o variable. This situation occurs in our results.

Thus, if $f_x \neq 1$, the local continuation of the family as a space-symmetric family is always defined and no intersections with families of the same period occur.

9.4.2 $f_x = 1$

The tangent equations reduce to:

$$\begin{bmatrix} 0 & f_C \\ g_x & g_C \end{bmatrix} \begin{bmatrix} dx_o \\ dC \end{bmatrix} = \begin{bmatrix} 0 \\ 0 \end{bmatrix} \tag{120}$$

$$\begin{bmatrix} f_{\dot{x}} & 0 \end{bmatrix} d\dot{x}_o = \begin{bmatrix} 0 & 0 \end{bmatrix}. \tag{121}$$

An immediate implication from Equation 113 is that:

$$g_x f_{\dot{x}} = o. \tag{122}$$

In general, both of these values will not be zero at the same time. An implication from Equation 114 is that:

$$g_x f_C = o. \tag{123}$$

Again, both of these values will not be zero at the same time (in general).

'J'here are two situations to consider here: $f_{\dot{x}} =$ O or $g_x =$ O. Wc assume that these situations are mutually exclusive.

First consider $f_{\dot{x}}$ = O and $g_x \neq$ O. Then $f_C =$ ***O*** also. The tangent equations may be reduced to:

$$g_x dx_o + g_C dC = \boldsymbol{O} \tag{124}$$

$$0 d\dot{x}_o = \boldsymbol{O}. \tag{125}$$

In this case a tangent, is still defined in the spat.e-sylnlrrctjric family of orbits:

$$dx_o = - \frac{g_C}{g_x} dC. \tag{126}$$

However the tangent direction $d\dot{x}_o$ is not unique, indicating that an intersection with a non-space symmetric family of equal period has occurred.

Next consider g_x = O and $f_{\dot{x}} \neq$ O. Then f_C and g_C need not be zero. The tangent equations become:

$$0dx_o = o \tag{127}$$

$$f_C dC = o \tag{128}$$

$$g_C\, dC = o \tag{129}$$

$$f_{\dot{x}} d\dot{x}_o = o. \tag{130}$$

First note that the tangent $d\dot{x}_o$ = O. Thus intersection with a non-symmetric family of the same period does not occur here. If $f_c = g_c =$ O then both dx_o and dC are free to vary and the tangent is not uniquely defined. This indicates that the family has intersected with another space-symmetric family of the same period. If either f_C or g_C are not zero then the result $dC =$ O follows. Then, in general, no intersection with another family has occurred and the tangent to the family is parallel to the x_o axis and is normal to the C axis, i.e. the family is passing through a local extremum with respect to the energy C.

9.4.3 $f_x = -1$

From the previous analyses the local continuation of the space-symmetric family is well defined at this critical point). '1'0 understand what occurs here consider the double composition of the monodromy matrix, effectively turning the periodic orbit into a periodic orbit with twice the period.

The tangent equations become:

$$\begin{bmatrix} 2(f_x^2 - 1) & f_C(f_x + 1) + f_{\dot{x}} g_C \\ 2f_x g_x & g_C(f_x + 1) + g_x f_C \end{bmatrix} \begin{bmatrix} dx_o \\ dC \end{bmatrix} = \begin{bmatrix} 0 \\ 0 \end{bmatrix} \tag{131}$$

$$\begin{bmatrix} 2f_x f_{\dot{x}} & 2(f_x^2 - 1) \end{bmatrix} d\dot{x}_o = \begin{bmatrix} 0 & 0 \end{bmatrix}. \tag{132}$$

For these equations only the case of $f_x = -1$ is of interest. Thus the equations reduce to:

$$\begin{bmatrix} 0 & f_{\dot{x}} g_C \\ -2g_x & g g_x f_C \end{bmatrix} \begin{bmatrix} dx_o \\ dC \end{bmatrix} = \begin{bmatrix} 0 \\ 0 \end{bmatrix} \tag{133}$$

$$\begin{bmatrix} -2f_{\dot{x}} & 0 \end{bmatrix} d\dot{x}_o = \begin{bmatrix} 0 & 0 \end{bmatrix} \tag{134}$$

The additional conditions are:

$$g_x f_{\dot{x}} = 0 \tag{135}$$

again both not zero at the same time.

If g_x = O then $d\dot{x} =$ O, $dC =$ O and dx is arbitrary. 'J'he]) intersection has occurred with a space-symmetric family of orbits with twice the period of the current family. The intersecting family is at a local extremum with respect to the energy.

If $f_{\dot{x}}$ = O then $d\dot{x}$ is arbitrary and $dx = \frac{1}{2} f_C dC$. Then intersection has occurred with a non-space-symmetric family with twice the period.

in these cases an extremum of the single period family with respect to the energy cannot occur as then $f_x = 1$ must have occurred, which contradicts the current hypothesis.

9.4.4 Catalog of **Possibilities**

Combining the above results yields a list of possible occurrences at the critical points. Only generic possibilities are listed.

$f_x = 1$, $g_x = 0$: If $f_C = g_C = 0$, intersection with a space-symmetric family of the same period has occurred. If either $f_C \neq$ O or $g_C \neq$ O, then the family is at a local extremum with respect to C.

$f_x = 1$, $f_{\dot{x}} = 0$: intersection with a non-space-symmetric family of the same period has occurred.

$f_x = -1$, $g_x = 0$: Intersection with a space-symmetric family of twice the period has occurred.

$f_x = -1$, $f_{\dot{x}} = 0$: Intersection with a non-space-symmetric family of twice the period has occurred.

We do not consider questions of continuation in the out-of-plane direction, although they may be of interest.

9.5 Presentation of Results

Members of the family of orbits have been computed for various values of σ. The families are presented as curves in tile (x_o, C) space in Figures 4 - 8. Figure 4 presents the curve for $\sigma =$ O. The periodic family in this case is just a straight, line traveling with a constant velocity in a downward direction for $x_o > 0$. Note that this family intersects the coordinate location $x_o =$ O, y_o = O at C = O. Because of this intersection the analytic continuation of this family to $\sigma > 0$ is complicated and would have to be studied with regularized equations of motion. **An** alternative to this would be to study the orbit using the Modified Hill equations where there is no singularity as $\sigma \rightarrow$ O. An investigation of the literature shows that this is a non-trivial case (Reference [1]]). Note that all the families are symmetric about x_o = O, thus only the results for $x_o >$0 arc given. **Also,** stability in the following paragraphs means stability of the orbit in the plane only. Out-of-Plane stability is briefly discussed later. In Figures 5- 8, stable portions of the families arc denoted by solid lines, unstable portions by dashed lines.

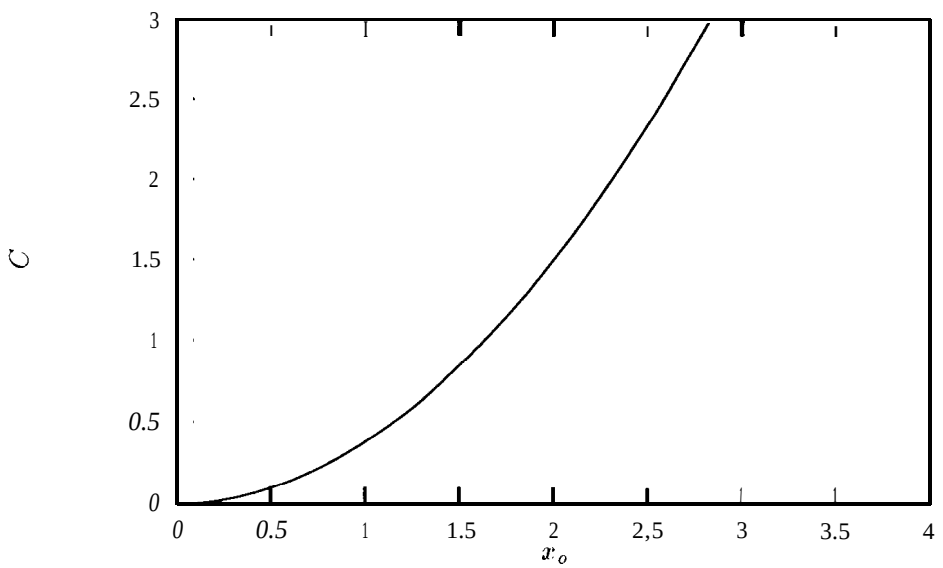

Figure 4: Symmetric Periodic Orbit Family: σ = O

As σ increases from O the family evolves. The evolution of this family may be explained as follows.

9.5.1 $\sigma > 0$

A few characteristics are evident for all the families with non-zero σ. First, as $x_o \to \infty$ the family curves become parabola in the (x_o, C) space.

The families are all stable for sufficiently large x_o. As x_o decreases the families become unstable via an intersection with an asymmetric periodic orbit of twice the period $(f_x = -1, f_{\dot{x}} = 0)$. Following this instability, the families may be discriminated according to whether or not σ is small enough, as will be discussed in a moment.

A common feature of all the families is that they reach an extremum with respect to x_o subsequent to their intersection with the asymmetric, doubly periodic orbit family. At, this extremum $g_x = 0$ while $g_C \neq 0$. After this extremum, the families have an increasing x_o while C continues to decrease.

Following this, the families again intersect an asymmetric doubly periodic orbit family $(f_x = -1, f_{\dot{x}} = 0)$ and regain stability. Then the families reach an extremum with respect to C $(f_x = 1, g_x = 0, f_C$ or $g_C \neq 0)$. At this point the family becomes unstable again. Subsequent to this the families begin to trace out a spiral in the (x_o, C) plane. An extremum with respect to x_o is followed by an extremum with respect to C, the process repeating indefinitely. After every local maximum of C and before every local minimum of C the families have small intervals of stability. These intervals decrease in size as the spiral grows tighter. It is conjectured that the spirals continue indefinitely.

Numerical continuation of the families becomes difficult at this point due to several effects. Due to accuracy limitations it becomes difficult to trace out a family in such a small region of the plane. Also, the periodic orbits in this region suffer extremely close encounters with the ring particles and may collide with them. '1'0 continue the family in this region would require that the equations of motion be regularized against, collision, a procedure that has not been done for this analysis.

9.5.2 $0 < \sigma <$ (71'

In analyzing the periodic orbit families another important value of σ has been found, denoted here by u],. The value of σ_L has been computed to within

$$0.01282 < \sigma_L < 0.01283 \tag{136}$$

and thus $\sigma_L < \sigma_{E3}$.

For rings with $\sigma < \sigma_L$ there is an interesting occurrence in these periodic orbit families. After the first intersection with the asymmetric double period family (when the family becomes unstable for the first time as x_o decreases), the families intersect an unstable, symmetric double period family $(f_x = -1, g_x = 0)$. The families then remain stable over an interval. This interval may include the first extremum with respect to x_o but terminates before the next intersection with the asymmetric double period family. The stable interval ends by re-intersecting the same unstable, symmetric double period family. In Figure 6 this unstable, symmetric double period family is denoted by a dotted line.

If $\sigma \ll \sigma_L$ the intervals between intersection with the asymmetric and symmetric double period families become vanishingly small. As σ grows larger the stable interval shrinks until $\sigma = \sigma_L$ when the unstable, symmetric double period family shrinks to a point.

The individual members of this stable interval are quite interesting. Figure 9 shows a few trajectories of members of this interval for $\sigma = 0.01$. Note that these trajectories pass very close to, and even encircle, the stable equilibrium point $E3$. Every family in this group $(\sigma < \sigma_L)$ contains such orbits that encircle the $E3$ points. As they are stable orbits, they may persist, under small perturbations. Also, the fact that they come c1 osc to a stable equilibrium point introduces some interesting possibilities concerning the manner in which a ring may gain mass. These mechanisms are discussed in more detail in Section 10.

9.5.3 $\sigma > \sigma_L$

For rings with a large enough value of σ the interval of stable orbits no longer exists. Current studies have investigated these families up to σ = us at which the ring itself becomes unstable.

It is interesting to note that no intersections of the families investigated with symmetric, single period families were found. The only intersection with a symmetric family found were those with the unstable, double period symmetric family for $\sigma < \sigma_L$. Furthermore, this intersection was closed as the double period symmetric family only intersected the single period symmetric family under consideration. The result being that these symmetric families of periodic orbits are isolated from all other symmetric families of a similar period, forming a closed group. Verification of this would require a complete investigat ion of the families as $\sigma \rightarrow$ O and in the spiral region of the families.

9.6 Out-of-Plane Stability

The out-of-plane stability characteristics of these families have also been computed. It is found that planar and out-of-plane stability coincide in most regions of interest: x_o >>0 and in the "stable interval". The only exception is within the stable interval where for a very small segment the families lose the out-of-plane stability, It is supposed that an intersection with an out-of-plane periodic orbit has occurred at these points. Such orbits would be of interest, to compute.

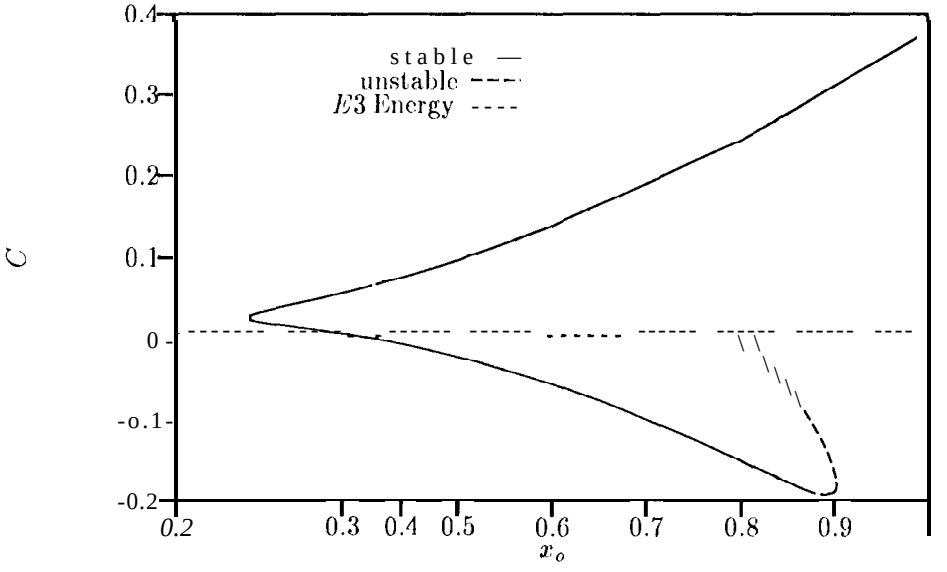

Figure 5: Symmetric Periodic Orbit Family: $\sigma = 0.001$

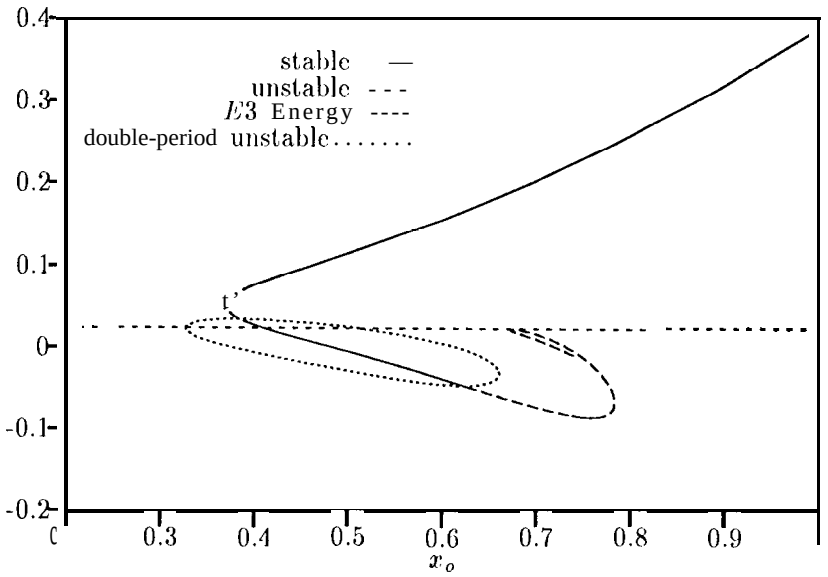

Figure 6: Symmetric Periodic Orbit Family: $\sigma = 0.01$

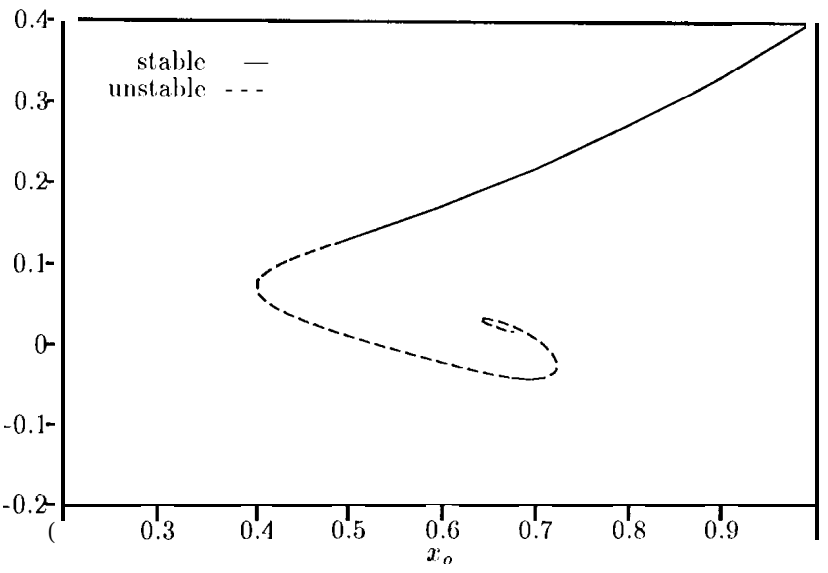

Figure 7: Symmetric Periodic Orbit Family: $\sigma = \sigma_{E3}$

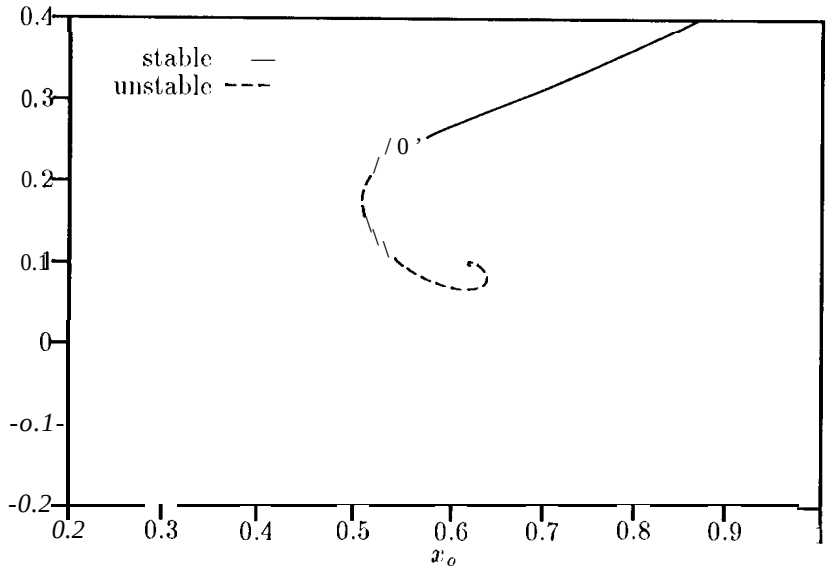

Figure 8: Symmetric Periodic Orbit Family: $\sigma = 0.07$

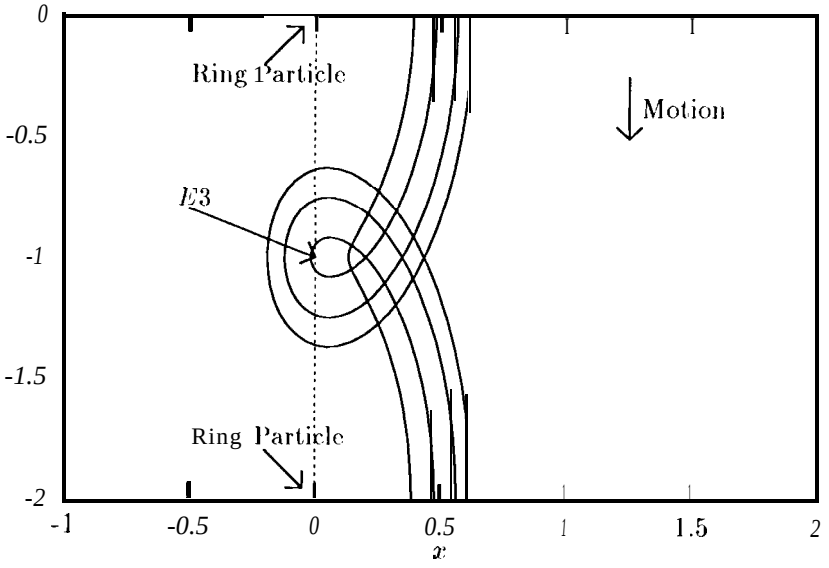

Figure 9: Stable Periodic Orbits: $\sigma = 0{,}01$

IO Mechanisms for a Ring to Gain Mass

Combining the results of the study of Equations 72, some simple observations may be made concerning the ability of a stable ring to gain mass. These observations are conjectural in nature and further analysis will be done to verify and/or refine them.

With such an elementary ring as being studied here there are only a few mechanisms by which the ring may gain mass. The first of these discussed has been discussed previously in the literature and, in general, would not apply to a riug as it leads asymptotically to the condensation of a ring into a few satellites (Reference [1 8]). The second of the mechanisms discussed is novel and arises directly from the current analysis. This mechanism may be apl)lic.able to rings as it provides a mechanism by which a stable ring may gaiu mass until it becomes sufficiently heavy (yet still stable) at which point the mechanism ceases to exist.

10.1 Direct Mass Gain by Ring Particles

The first mechanism operates by assuming that the misting riug particles attract smaller particles and, via inelastic collisions with the small particles, grow in mass. In terms of the original formulation of the model as 1' ring particles of mass μ each, the mass μ will increase and the number of particles 1' will be fixed.

If continued, the result of this mechanism will eventually be $\mu > \mu_S$ and hence the P particle ring will become unstable. In the absence of neighboring rings this configuration has its greatest instability in the angular direction, hence instability will lead to collisions among the ring particles (Reference [16], Section 3.4.10). Assume that with the passage of time the ring is able to re-stabilize itself. It is of interest to know whether the number and mass of particles has increased or decreased.

Let the original, unstable, ring have P_1 particles each of mass μ_1, where $\mu_1 > \mu_S(P_1)$. If the final, assumed stable, configuration has P_2 particles each of mass μ_2, then the following mass conservation law will hold:

$$\mu_1 1', \quad = \quad \mu_2 P_2 \tag{137}$$

Furthermore, the masses μ_1 and μ_2 can be related by a factor r: $\mu_2 = r\mu_1$ Thus $P_2 = 1/rP_1$. Assume that the new ring is stable, $\mu_2 < \mu_S(P_2)$. Next note that,:

$$\begin{aligned} \mu_S(P_2) &= /\mathrm{is}(\mathrm{I'l} \quad /?') \\ &= r^3 \mu_S(P_1) \end{aligned} \tag{138}$$

Then it is easy to verify that $r > 1$. Hence $1'2 < 1'1$ and $\mu_2 > \mu_1$, or to stabilize the ring must rearrange itself into a riug with fewer, heavier particles. Iteration of this process would reduce a ring to a few, massive particles. At this point it should be noted that a classical riug (as defined here) with $P \leq 7$ is always unstable, independent of the mass (References [10], [12], [13]). However, for 1'$ 10 other stable, non-symmetric configurations exist. See Reference [1 2] for au in-depth discussion of the dynamics in such a system.

From the shove discussion it is clear that such a mechanism dots not apply to rings. It may, however, apply to satellite formation about a planet or a star.

10.2 Mass Gain About Stable Equilibrium Points

The second mechanism is nove1 and arises from the current analysis. This mechanism is applicable to the study of rings in that it allows a ring to gaiu mass if sufficiently small, yet is also self-li]llitillg in that it does not allow a ring to become so massive that it becomes unstable. The rudiments of the theory are sketched here, yet require more research to verify and refine the actual mechanism.

At the heart of this mechanism is the supposition that a stable ring as posited here exists, and that a sufficient amount of small particles orbit close to the ring. As discussed in Section 9.3 there are stable orbits which lie on either side of the ring at a sufficient distance x_o from the ring. Also, if $\sigma < \sigma_L$, there are stable orbits which pass through the vicinity of the $E3$ equilibrium points (whit.11 are stable for this value of σ). As observed in Figure 9, these orbits intersect themselves and each other in the vicinity of the $E3$ points. Also important to point out is that tile mirror images of these periodic orbits exist and will also interact, in the vicinity of the $E3$ points. Thus, if small particles follow these stable orbits, they are given the opportunity to interact in the vicinity of the $E3$ equilibrium points.

Assume a dissipative interaction between the small particles in the vicinity of the $E3$ points. A likely mechanism might be inelastic collisions. Then the kinetic energy of the particles with respect to the rotating ring will decrease, i.e. $dT' < 0$ where:

$$T' = \frac{1}{2}(\dot{x}^2 + \dot{y}^2) . \tag{139}$$

With reference to the energy integral (Equation 47) it becomes apparent that $dC > 0$, or that the energy parameter C will increase. As seen on the periodic orbit family plots (Figures 5 and 6), this will cause the energy of the small particles to approach the energy of tile stable E3 point. The fact that these periodic. orbits are stable is important as it allows for the particles to oscillate around the families and to travel along the family curve as the energy parameter C increases. As the particles approach the geometric position and the energy value of the $E3$ points, it becomes possible for them to become trapped about the stable equilibrium point.

Continuing this process, the accumulated mass of the small particles at the E3 points may increase to the point where the total mass in the vicinity of these points equals σ. Then the ring system is similar to the original system, although containing twice the particles. At this stage of the scenario the ring particles are located at the coordinates $(x_k = 0,\ y_k = k, z_k = 0);\ k = 0, \pm 1, \ldots$. The equations of motion of a small particle are then:

$$\begin{aligned} \ddot{x} - 2\dot{y} &= V_x \\ \ddot{y} + 2\dot{x} &= V_y \\ \ddot{z} &= V_z \end{aligned} \tag{140}$$

$$V(x,y,z) = \frac{3}{2}x^2 - \frac{1}{2}z^2 + \frac{\sigma}{\sqrt{x^2 + y^2 + z^2}} + \sigma \sum_{k=-\infty}^{\infty}{}' \left[\frac{1}{\sqrt{x^2 + (k-y)^2 + z^2}} - \frac{1}{|k|} \right] . \tag{141}$$

Note that the potential function is different from the one given in equation 73. To put these equations back into the standard form of the Close Ring equations make the transformation:

$$(x, y, x) \rightarrow \left(\frac{1}{2}x, \frac{1}{2}y, \frac{1}{2}z\right) . \tag{142}$$

In carrying out this transformation the parameter σ is modified and becomes 8σ. Thus the new ring has effectively increased its mass parameter σ by a factor of 8. The new ring has also increased its region of influence, especially in the x direction where it has doubled via the scaling transformation. Thus new regions of small particles adjacent to the ring are available to be captured at the new stable E3 points.

Note that this process cannot be continued indefinitely. Starting from a ring with mass σ_0, at the nth stage of the cycle the ring mass parameter will have a value $\sigma_n = 8^n \sigma_0$. At some point $\sigma_n > \sigma_L$ will occur. Then the proposed mechanism of deposition, the stable orbits which pass close

to the stable $E3$ points, will cease to exist aud become unstable orbits. Also, as $\sigma_L < \sigma_{E3} < \sigma_S$, the ring itself will still be stable at this point.

This mechanism is attractive as it sketches out how a ring, once started, may grow in size by capturing neighboring particles. Also, as it is a self-limiting process, the end result is a riug stable with respect to self-gravitation.

With the basic mechanism sketched out, it also becomes apparent what issues must be addressed to verify the assumptions and to refine the process. A few of these items are listed below:

- Derive plausible mechanisms for particles to jump from the stable periodic orbits encircling $E3$ to orbits trapped near $E3$. Possible mechanisms include collision effects, viscous effects, or self at, traction of the particles going through the slow portion of the orbit encircling E3 (note that the kinetic energy is minimized along this portion of the orbit). Any mechanism that dissipates velocity while the particle is encircling $E3$ may be a candidate mechanism.

- Study the stability of a hybrid ring solution described as follows. Consider the nominal ring solution of P particles of mass μ. Consider the hybrid solution defined by introducing P additional particles, of mass less than μ, in the vicinity of the $E3$ equilibrium point. It cau be shown that such a solution exists. Two limiting results for such a system arc already known. If the additional 1' particles are massless, then the upper bound on μ for the riug to be stable is $\frac{1}{4}\mu s(P)$. If the additional P particles have mass μ, then the upper bound on μ for the ring to be stable is $\frac{1}{8}\mu s(P)$. A reasonable conjecture is that the upper bound for stability in the intermediate cases will vary continuously from the one limit to the other. Nonetheless this must be verified.

- The Close Ring equat ions of motion can be easily modified to model the hybrid ring case mentioned above. What must, be investigated is whether stable periodic orbits still exist, whit.]] can deposit, particles onto the smaller masses, eventually increasing their mass till they are approximately equal to the original ring particle mass.

- Note that the above hybrid ring cases may uot need to be considered if the particle accretion rate at $E3$ is fast enough. If this is so, then the time frames involved may be short enough so that the hybrid case never has opportunity to affect the mechanism. Thus, some measure of the time required for particle accretion is required.

11 Conclusions

A simplified dynamical model has been derived which describes the dynamics of small particles as attracted by a ring. Important results include a rigorous modification to the Hill equations of motion which includes the effects of neighboring particles. Also, a substantively new model for the motion of small part, icles close to a ring is derived and examined. This model does not include non-gravitational forces which may play an important role in particle dynamics near a ring. Using this new model, a possible mechanism for riug growth was identified. This mechanism is of interest as it is self-lilnit,ing in that it ceases to operate when the ring becomes heavy enough, yet while the ring is still gravitationally stable. Future issues to investigate are also identified.

Acknowledgements

This research was performed in part at the University of Michigan under the support of a Rockwell Fellowship.

A Application of the Limit in the Close Ring Equations

In this appendix the limit described in Section 4 is applied to the ring force terms (Equations 29 - 31), yielding the modified ring force terms (Equations 34- 36).

The limit is applied using the following result for a fixed integer k:

$$\lim_{\theta \to 0} \frac{\sin \theta k}{\theta} = k. \tag{143}$$

Using this limit the following results hold:

$$\lim_{\theta \to 0} \frac{\sin^2 \theta k}{\theta} = 0 \tag{144}$$

$$\lim_{\theta \to 0} \frac{\sin \theta k \cos \theta k}{\theta} = k \tag{145}$$

$$\lim_{\theta \to 0} |\mathbf{r}_k| = \sqrt{\hat{x}^2 + \left(\frac{2k}{\chi \sigma^{1/3}} - \hat{y}\right)^2 + \hat{z}^2} \tag{146}$$

where

$$|\mathbf{r}_k| \cdot \sqrt{\frac{4 \sin^2 \theta k}{\sigma^{2/3} \chi^2 \theta^2} - \frac{4 \sin \theta k}{\sigma^{1/3} \chi \theta} (\hat{y} \cos \theta k - \hat{x} \sin \theta k) + \hat{x}^2 + \hat{y}^2 + \hat{z}^2}. \tag{147}$$

The problem in applying the limit to the summation is that there are always values of k large enough (on the order of $P/2$) so that the limit 143 is invalid. It is seen, however, that the contribution of these terms to the summations will vanish under application of the limit. Consider the worst case scenario. Let $P = 2r$ and $k = r$. Then for $\theta << 1$ the approximate results are:

$$\frac{1}{|\mathbf{r}_r|^3} = \frac{\sigma \chi^3}{8} \pi \left(\frac{3}{2r}\right). \tag{148}$$

Using the limit approximation (Equation 143) the approximate value is:

$$\frac{1}{|\mathbf{r}_r|} = \frac{\sigma \chi^3}{8} \frac{1}{r^3}. \tag{149}$$

Consider the difference of these terms:

$$\frac{\sigma \chi^3}{8 r^3} \left[\left(\frac{\pi}{2}\right)^3 - 1\right]$$

As the parameter $r \to \infty$ the difference between these terms goes to zero.

The more general result is derived as follows. For all finite values of $\hat{x}, \hat{y}, \hat{z}$ and for k large enough and O small enough the quantities $|\mathbf{r}_k|$ take on the asymptotic form:

$$|\mathbf{r}_k| \approx \frac{2}{\sigma^{1/3} \chi} \frac{\sin \theta k}{\theta}. \tag{150}$$

Since it is under these conditions (k large) that, the limit dots not hold it is of interest to compute the basic summation:

$$\sum_{r_1}^{r_2}{}' \frac{1}{|\mathbf{r}_k|^3} = \sum_{r_1}^{r_2}{}' \frac{\theta^3}{\sin^3 \theta k} + \mathcal{O}(\theta) \tag{151}$$

using both the limit approximation and exact, asymptotic results. Using Approximation 143 the result is:

$$\lim_{\theta \to 0} \sum_{r_1}^{r_2}{}' \frac{\theta^3}{\sin^3 \theta k} = 2\zeta(3) \tag{152}$$

where $\zeta(n)$ is the Riemann Zeta formula as described previously.

Now consider the exact result,. First the summation may be rewritten as:

$$\sum_{r_1}^{r_2}{}' \frac{\theta^3}{\sin^3 \theta k} = \sum_{1}^{P-1} \frac{\theta^3}{\sin^3 \theta k} \tag{153}$$

Trigonometric substitution will show that:

$$\sum_{1}^{P-1} \csc^3 \theta k = \frac{1}{2} \sum_{1}^{P-1} \csc^3 \theta k (1 + \cos^2 \theta k) + \frac{1}{2} \sum_{1}^{P-1} \csc \theta k. \tag{154}$$

These sums may be found asymptotically (Reference [1 3], Appendix):

$$\sum_{1}^{P-1} \csc^3 \theta k (1 + \mathrm{COS}^2 \theta k) = \frac{4(3)}{\theta^3} + \mathcal{O}(1/\theta) \tag{155}$$

$$\sum_{1}^{P-1} \csc \theta k = \frac{1}{\theta} \log\left(\frac{4 \exp \gamma}{\theta}\right) + \mathcal{O}(\theta). \tag{156}$$

'1'bus:

$$\sum_{r_1}^{r_2}{}' \frac{\theta^3}{\sin^{33} \theta k} = 2<(3) + \mathcal{O}(\theta^2). \tag{157}$$

Applying the limit O → O then yields the previous result, establishing the validity of the limit.

References

[ ]] B. Chauvineau & F. Mignard, "Dynamics of Binary Asteroids. 1.", Icarus, Vol 83, pp 360-381, 1990.

[2] F. Delhaise & M. Moous, "Effects of a Non-Circular Shepherd Upon a Planetary Riug", pp 173-180 iu Long-Term Dynamical Behavior of Natural and Artificial N-Body Systems, A .E. Roy, editor, Kluwer Academic, 1988.

[3] M. Hénon, "Exploration Numérique du Problème Restreint. 11.", Annales D'Astrophysique, Vol 28, No 6, pp 992-1007, 1965.

[4] M. Hénon, "Numerical Exploration of the Restricted Problem. V.", Astronomy and Astrophysics, Vol 1, pp 223-238, 1969.

[5] M. Hénon, "Numerical Exploration of the Restricted Problem. VI .", Astronomy aud Astrophysics, Vol 9, pp 24-36, 1976.

[6] M. Hénon & J.-M. Petit, "Series Expa nsions for Encounter-Type Solutions of Hill's Problem", Celestial Mechanics, Vol 38, pp 67-100, 1986.

[7] C. Marchal, The Three-Body Problem, Elsevier, 1990.

[8] J.C. Maxwell, Scientific_Papers, Dover, 1952.

[9] K.R. Meyer & D.S. Schmidt, "Librations of Central Configurations and Braided Saturn Rings", Celestial Mechanics, Vol 55, No 4, pp 289-303, 1993.

[10] C.G.Pendse, "The Theory of Saturn's Rings", Philisophical Transactions of the Royal Society, Series A, Vol 234, pp 145-176.

[11] J.-M. Petit & M. Hénon, "Satellite Encounters", Icarus, Vol 66, pp 536-555, 1986.

[12] H. Salo & C.F. Yoder, "The Dynamics of Coorbital Satellite Systems", Astronomy and Astrophysics, Vol 205, PP 309-327, 1988.

[13] D.J. Scheeres & N.X. Vinh, "Linear Stability of a Self-[gravitating Ring", Celestial Mechanics, Vol 51, pp 83-103, 1991.

[14] D.J. Scheeres & N.X. Vinh, "The Restricted 1' + 2 Body Problem", Acta Astronautica, Vol 29, No 4, pp 237-248, 1993.

[15] D.J. Scheeres & N.X. Vinh, "The Restricted Hill Four-Body Problem", paper IAF-92-0006, presented at the World Space Congress, Washington D.C., 1992.

[16] D.J. Scheeres, On Symmetric Central Configurations with Application to Satellite Motion About Rings, Doctoral Dissertation, The University of Michigan, 1992.

[17] J. Waldvogel & F. Spirig, "Co-Orbital Satellites and Hill's Lunar Problem", PP 223-234 in Long-Term Dynamical Behavior of Natural and Artificial N-Body Systems, A.E. Roy editor, Kluwer Academic, 1988.

[18] E. Willerding, "Theory of Density Waves in Narrow Planetary Rings", Astronomy and Astrophysics, Vol 161, pp 403-407, 1986.

[19] A. Wintner, The Analytical Foundations of Celestial Mechanics, Princeton University Press, 1947.